

We are IntechOpen, the world's leading publisher of Open Access books Built by scientists, for scientists

4,800

Open access books available

122,000

International authors and editors

135M

Downloads

Our authors are among the

154

Countries delivered to

TOP 1%

most cited scientists

12.2%

Contributors from top 500 universities



WEB OF SCIENCE™

Selection of our books indexed in the Book Citation Index
in Web of Science™ Core Collection (BKCI)

Interested in publishing with us?
Contact book.department@intechopen.com

Numbers displayed above are based on latest data collected.

For more information visit www.intechopen.com



Hydrogenation of Graphene and Hydrogen Diffusion Behavior on Graphene/Graphane Interface

Zhimin Ao and Sean Li

*School of Materials Science and Engineering
The University of New South Wales, Sydney, NSW 2052
Australia*

1. Introduction

Hydrogenation of carbon materials has been attracting a wide range of interests as an application of hydrogen storage materials in hydrogen-powered automobile as well as a methodology to manipulate the electric properties of carbon materials. Graphene with unique electronic, thermal and mechanical properties has been investigated as one of the most promising candidates for the next generation of electronic materials (Geim, 2009). However, several major challenges have to be tackled before the widespread application of graphene. For example, the absence of a band gap in the electronic spectrum of intrinsic graphene and the Klein paradox as a consequence of the Dirac-type nature of the charge carriers (Novoselov et al., 2004; Rao et al., 2009). The most efficient way to overcome these problems is hydrogenation of graphene (Luo et al., 2009). The graphane (Sofa et al., 2007), a fully hydrogenated single layer of graphene, was suggested to possess the promising semiconductor properties with a band gap of around 3.5 eV theoretically. Very recently, Elias *et al.* (Elias et al., 2009) experimentally demonstrated the formation of graphane through the exposure of a graphene membrane to hydrogen plasma. Subsequently, the rate of hydrogenation process of multilayer graphene was found to strongly depend on the number of layers (Luo et al., 2009; Ryu et al., 2008). These discoveries open important perspectives for the application of graphene-based devices because the electronic gap in those graphanes could be controlled by the degree of hydrogenation (Elias et al., 2009; Zhou et al., 2009).

The hydrogenation process of graphene in above experiments occurs through the exposure of graphene to the hydrogen plasma, which contains H^+ , H_3^+ , H atoms and H_2 molecules (Elias et al., 2009; Luo et al., 2009). One generally assumes that H atoms form covalent bonds with the carbon atoms in the graphene (Luo et al., 2009). In this chapter, alternative approaches to hydrogenate graphene will be proposed theoretically based on density functional theory (DFT) calculations. It suggests that the hydrogenation process can be realized through the exposure of graphene to molecular hydrogen gas in the presence of a strong perpendicular electric field. It has been demonstrated that an electric field can modify the chemical activity of materials (Liu et al., 2009). For example, the dissociation activation energy of molecular oxygen on Pt (111) is tunable by an applied electric field (Hyman et al.,

2005). To understand the mechanism of graphene hydrogenation with molecular hydrogen, the pathway of the dissociation of a H₂ molecule and the subsequent atomic adsorption on graphene in the presence of an electric field will be investigated.

On the other hand, it is believed that graphene nanoribbons (GNRs) offer the possibility to achieve tunable electronic properties. This is because their properties are highly dependent on their width and also the orientation of edges, for example, the GNRs can be turned from semiconducting to metallic by manipulating the structural parameters (Han et al., 2010; Jiao et al., 2010). Unfortunately, to manipulate the edge structure and width of freestanding GNRs is a very challenging experimental task (Han et al., 2010; Jiao et al., 2010). Both experimental data and the corresponding *ab initio* calculations demonstrated that the zigzag edge is metastable in vacuum due to a planar reconstruction to lower the energy of the system (Koskinen et al., 2009). Alternatively the high quality GNRs can be fabricated by selectively hydrogenating the graphene or by carving GNRs on a graphane sheet (Balog et al., 2010; Sessi et al., 2009; Singh et al., 2009). A bandgap opening in graphene, induced by the patterned absorption of atomic hydrogen, was recently found experimentally (Koskinen et al., 2009). Meanwhile, the hybrid graphene/graphane nanoribbons (GGNRs) were also studied by *ab initio* calculations (Hernández-Nieves et al., 2010; Lu et al., 2009; Singh et al., 2010). It was shown that the bandgap of GGNRs is dominated by the graphene rather than the graphane (Hernández-Nieves et al., 2010; Lu et al., 2009; Singh et al., 2009). Its electronic and magnetic properties strongly depend on the degree of hydrogenation of the interface (Hernández-Nieves et al., 2010). However, the hydrogen diffusion associated with high mobility of the isolated H atoms on graphene has a strong influence on the stability of the graphene/graphane interface.

In this chapter, in order to enhance the hydrogen storage capacity in graphene and also to manipulate the electronic properties of graphene, the hydrogenation of graphene with and without an applied electric field, as well as the stability of the graphene/graphane interface in the hybrid nanoribbons are studied through DFT calculations. The energy barriers for the hydrogenation reaction and the diffusion of H atoms located at the graphene/graphane interface are simulated using DFT. All the possible reaction and diffusion pathways are analyzed to find the minimum reaction and diffusion barriers.

2. Hydrogenation of graphene

2.1 Hydrogenation of pristine graphene

In the simulation, all DFT calculations are implemented in the DMOL3 code (Delley, 2000). The local density approximation (LDA) with the PWC functional is employed as the exchange-correlation functional (Perdew & Wang, 1992). A double numerical plus polarization (DNP) is employed as the basis set. The convergence tolerance of energy is taken 10⁻⁵ Ha (1 Ha = 27.21 eV), and the maximum allowed force and displacement are 0.002 Ha and 0.005 Å, respectively. To investigate the minimum energy pathway for the hydrogen dissociative adsorption on graphene, linear synchronous transition/quadratic synchronous transit (LST/QST) (Halgren & Lipscomb, 1977) and nudged elastic band (NBE) (Henkelman & Jonsson, 2000) tools in DMOL3 code are used, which have been well validated to find the structure of the transition state (TS) and the minimum energy pathway. In the simulation, three-dimensional periodic boundary conditions are taken. The computer simulation cell consists of a 2×2 graphene supercell with a vacuum width of 18 Å to minimize the interlayer interaction. The *k*-point is set to 20×20×1, and all atoms are allowed to relax.

The adsorption energy of a molecular H_2 on a pristine graphene layer E_{b-H_2} is defined as,

$$E_{b-H_2} = E_{H_2\text{-graphene}} - (E_{\text{graphene}} + E_{H_2}) \quad (1a)$$

where $E_{H_2\text{-graphene}}$, E_{graphene} , E_{H_2} denote the energy of the system with a H_2 molecule adsorbed on graphene, the energy of the graphene layer and a H_2 molecule, respectively. For the case of atomic H chemically bonded on pristine graphene, the binding energy E_{b-H} is defined as,

$$E_{b-H} = [E_{2H\text{-graphene}} - (E_{\text{graphene}} + 2E_H)] / 2 \quad (1b)$$

where $E_{2H\text{-graphene}}$ is the energy of the system with 2 H atoms bound on the graphene layer, E_{graphene} is the energy of the graphene layer, and E_H is the energy of a free H atom in the same slab lattice.

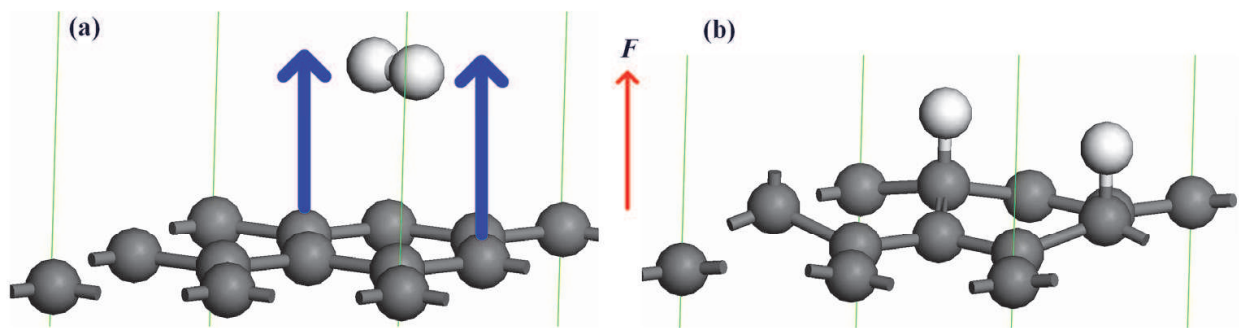


Fig. 1. The initial (panel a) and final (panel b) structures for a H_2 molecule dissociative adsorption on graphene. In this figure, a 2×2 supercell is shown where the gray and white balls are carbon and hydrogen atoms, respectively. The direction of the electric field is indicated by the arrow. (Reproduced with permission from Ref. (Ao & Peeters, 2010a). Copyright 2010, AIP)

For the case of molecular hydrogen adsorbed on graphene, previous DFT reports showed that the H_2 molecule is weakly physisorbed at the hollow site of graphene as shown in Fig. 1(a) (Ao et al., 2009, Arellano et al., 2000). The distance between the H_2 molecule and the graphene layer $d_{H_2\text{-graphene}}$ is 2.612 \AA with adsorption energy $E_{b-H_2} = -0.153 \text{ eV}$, which are consistent with other simulation results of $d_{H_2\text{-graphene}} = 2.635 \text{ \AA}$ and $E_{b-H_2} = -0.159 \text{ eV}$ (Ao et al., 2009), and $d_{H_2\text{-graphene}} \approx 2.8 \text{ \AA}$ and $E_{b-H_2} = -0.133 \text{ eV}$ (Okamoto et al., 2001). For the case of atomic hydrogen adsorption on graphene, the favorable configuration is two H atoms adsorbed on two face-by-face carbon atoms in the same hexagon as shown in Fig. 1(b), which is consistent with the reported DFT result (Miura et al., 2003). The C-H bond length l_{C-H} is 1.125 \AA with binding energy $E_{b-H} = -2.184 \text{ eV}$, which agrees with another DFT result $l_{C-H} = 1.13 \text{ \AA}$ (Miura et al., 2003). In addition, the C atoms bonded with the two H atoms move up towards the H atoms with about 0.32 \AA and the C-C bond length l_{C-C} is 1.493 \AA . This is similar to the sp^3 bond length of 1.53 \AA in diamond while it is much longer than 1.420 \AA for the sp^2 carbon length. The reconstruction of the graphene layer was also reported by the others, in which the C atoms bonded with the H atoms move out of the graphene plane by 0.35 \AA (Miura et al., 2003). In this case, the carbon hexagon becomes more chemically active as it turns from sp^2 bonding to sp^3 like bonding (Miura et al., 2003). Based on the calculation of the band structure for the structure shown in Fig. 1(b), this hydrogenated graphene has a band gap of 3.4 eV , which is consistent with that of 3.5 eV for fully hydrogenated graphene – graphane (Sofa et al., 2007).

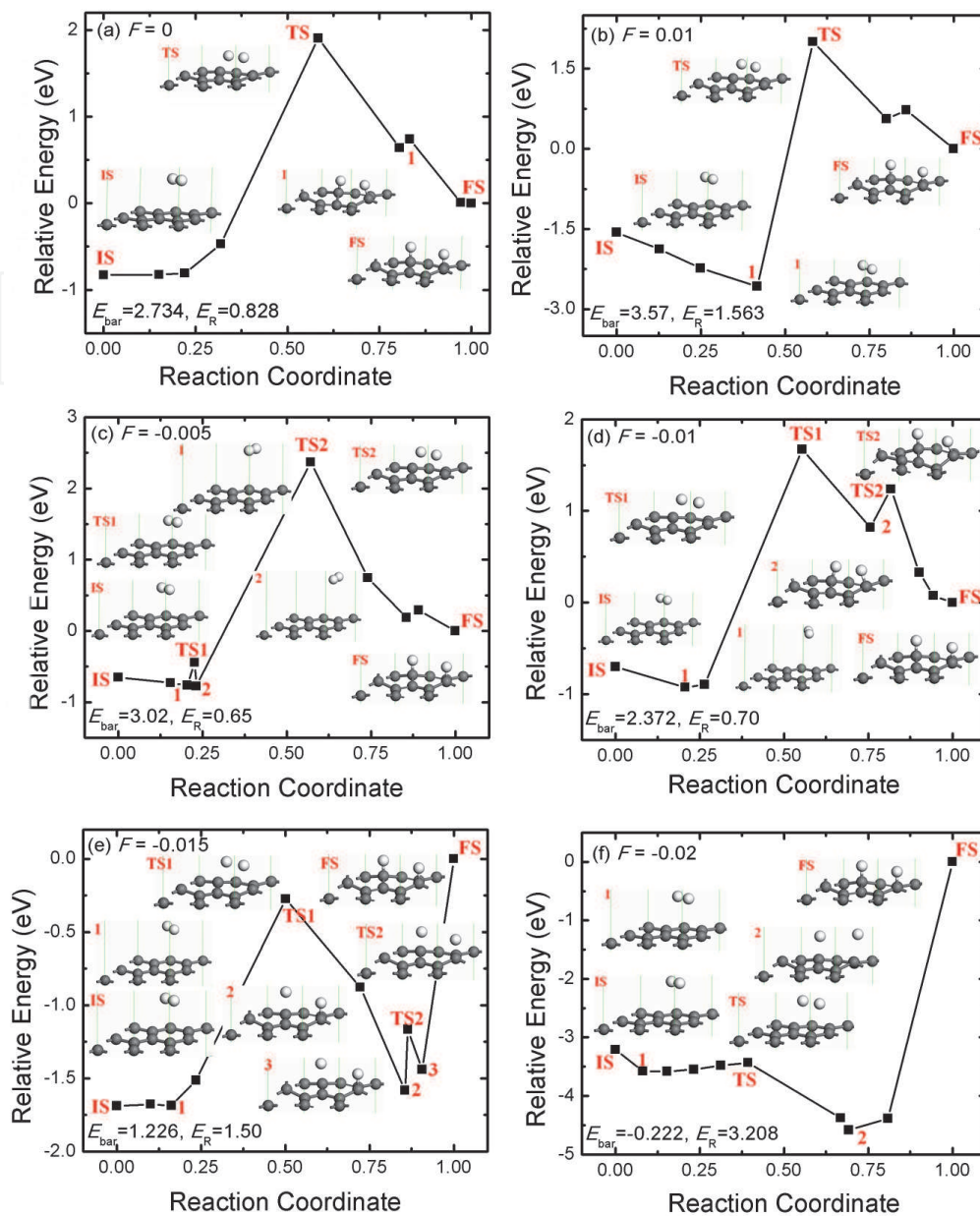


Fig. 2. The reaction pathway of a H_2 molecule that undergoes a dissociative adsorption on graphene for different electric field. IS, TS, FS, 1 and 2 represent initial structure, transition structure, final structure, energy minimum state 1 and 2, respectively. Their atomic structures are given by the inserts. The energy of FS is taken to be zero. The unit of F , E_{bar} and E_R are a.u. and eV, respectively, where E_{bar} is the energy barrier and E_R is the reaction energy. (Reproduced with permission from Ref. (Ao & Peeters, 2010a). Copyright 2010, AIP)

The energy minimum pathway for a H_2 molecule dissociative adsorption on graphene is from the structure depicted in Fig. 1(a) to the structure in Fig. 1(b), which agrees with the reported minimum pathway (Miura et al., 2003). Here, this dissociative adsorption pathway is shown in Fig. 2(a). From Fig. 2(a), the dissociative adsorption reaction barrier E_{bar} is 2.734 eV, which is smaller than 3.3 eV as reported (Miura et al., 2003). Regarding the transition state (TS), the H_2 molecule is dissociated into 2 free H atoms without any binding with the C atoms. After TS, these 2 H atoms bind with the C atoms and move to the exact top sites of

the C atoms shown as the final structure (FS) in Fig. 2(a). Thus, this is a two-step reaction. Step one is that the H₂ molecule is dissociated into 2 free H atoms. Subsequently, the 2 H atoms are bound to the two C atoms. Step one needs an energy of 2.7 eV to overcome the potential barrier and the second step releases an energy of 1.9 eV. So totally the reaction energy is about 0.8 eV for the H₂ dissociative adsorption on graphene. The dissociation of H₂ is the rate-limiting step because a large energy is required.

Next the effect of an electric field F on this dissociative adsorption process is investigated, our numerical results are shown in Fig. 2. From the figure, in general E_{bar} increases with increasing F , and the reaction energy E_R increases as the absolute value of F increases. However, there is an abnormal energy barrier value $E_{\text{bar}} = 3.020$ eV at $F = -0.005$ a.u., which is larger than those for $F = -0.01$ a.u. and $F = 0$ (1 a.u. = 5.14×10^{11} V/m). The physical interpretation of this abnormal E_{bar} value for $F = -0.005$ a.u. will be given later. Thus, such a negative electric field can act as a catalyst to significantly facilitate the hydrogenation process of graphene. However, E_R increases as E_{bar} decreases with increasing absolute value of the negative electric field. In order to confirm the occurrence of hydrogenation reaction, the change of the Gibbs free energy $\Delta G = \Delta H - T\Delta S$ is considered where ΔH , T and ΔS are the change of enthalpy, the reaction temperature and the change of entropy, respectively. From Fig. 2, one can see that the energies of the product are higher than those of reactant. So this hydrogenation process is an endothermic reaction, i.e. $\Delta H > 0$. On the other hand, molecular H₂ is dissociated into two H atoms, this step leads to an increase of entropy, e.g. $\Delta S > 0$. Thus, if sufficient energy is available, which is the case at high temperature, ΔG can become negative and the reaction will go smoothly and efficiently.

The pathways for this reaction under different electric fields are given in Fig. 2. The energy minimum atomic structures of both reactant and product change in the presence of an electric field (Ao et al., 2008b). As shown in Fig. 2(b) at $F = 0.01$ a.u., the reactant was geometry optimized from the initial structure (IS) to the energy minimum state - State 1, where the physisorbed H₂ molecule moves towards the carbon layer while a negative electric field pushes the H₂ molecules upwards as shown in Figs. 2(c)-2(e). Under $F = -0.02$ a.u. as shown in Fig. 2(f), the H₂ molecule in the reactant is dissociated into two free H atoms as indicated by State 1. On the other hand, the energies of FS in Figs. 2(e) and 2(f) are not minimal after the TS. Thus the reaction will be terminated at State 2 in both Figs. 2(e) and 2(f) if there is not sufficient energy available. At State 2 in Figs. 2(e) and 2(f), the H₂ molecule is already dissociated. The free H atoms are considered to automatically bind with the C atoms once the applied electric field is removed since there is no potential barrier after H₂ dissociation at TS as shown in Fig. 2(a). In addition, experiments have indicated that the graphene layer can be automatically hydrogenated by free H atoms (Elias et al., 2009; Luo et al., 2009). Notice that a negative E_{bar} -0.222 eV is found when $F = -0.02$ a.u.. In the other words, the reaction from IS to State 2 can automatically progress when $F = -0.02$ a.u., and subsequently we remove the electric field in order that the H atoms bind to the C atoms. In addition, in case of Fig. 2(c) there is an extra energy barrier before reaching the transition state of the whole reaction TS2, which may be the reason behind the appearance of abnormal E_{bar} value.

The origin of the changes in E_{bar} with F can be understood through the analysis of the partial density of states (PDOS). Fig. 3 shows the PDOS of hydrogen and the p orbital of the carbon atoms at which the H₂ molecule is dissociated and the H atoms are adsorbed. It is noted that the PDOS for both C and H atoms are changed. In general, the weight of the bands corresponding to the H atoms below the Fermi level increases as $-F$ increases, while those of the C atoms decreases. These changes are induced by the electron transfer between the H

and the C atoms. In the presence of a negative electric field, electrons flow from the C atoms at the bottom to H atoms at the top, and more charge is transferred as $-F$ increases. The strength of the interaction and the trend in E_{bar} can be explained by considering the positions and weights of the interaction between the bands of carbon and hydrogen. Based on the position of the bands, it is possible to identify the character of the C-H bands. The lowest C-H band around $-8 \sim -10$ eV are due to the interaction of the H σ_g state and the C P_z state (Zhang & Cho, et al., 2007). The second lowest C-H band around $-3 \sim -5$ eV is most likely related to the bonding interaction of H σ_u and C P_z states as they are above the H σ_g state. The H σ_u and the antibonding C P_z states above the Fermi level result in the highest C-H band, which determines the strength of the interaction and thus determines the energy barrier heights of the transition states (Arellano et al., 2000). As one can see from Figs. 3(e) and 3(f), the PDOS of the highest C-H bands are depressed and the lowest and the second lowest C-H bands are strongly enhanced. This agrees with the result in Fig. 2 that the barrier decreases to 1.226 eV at $F = -0.015$ a.u. and a negative E_{bar} -0.222 eV is found at $F = -0.02$ a.u.

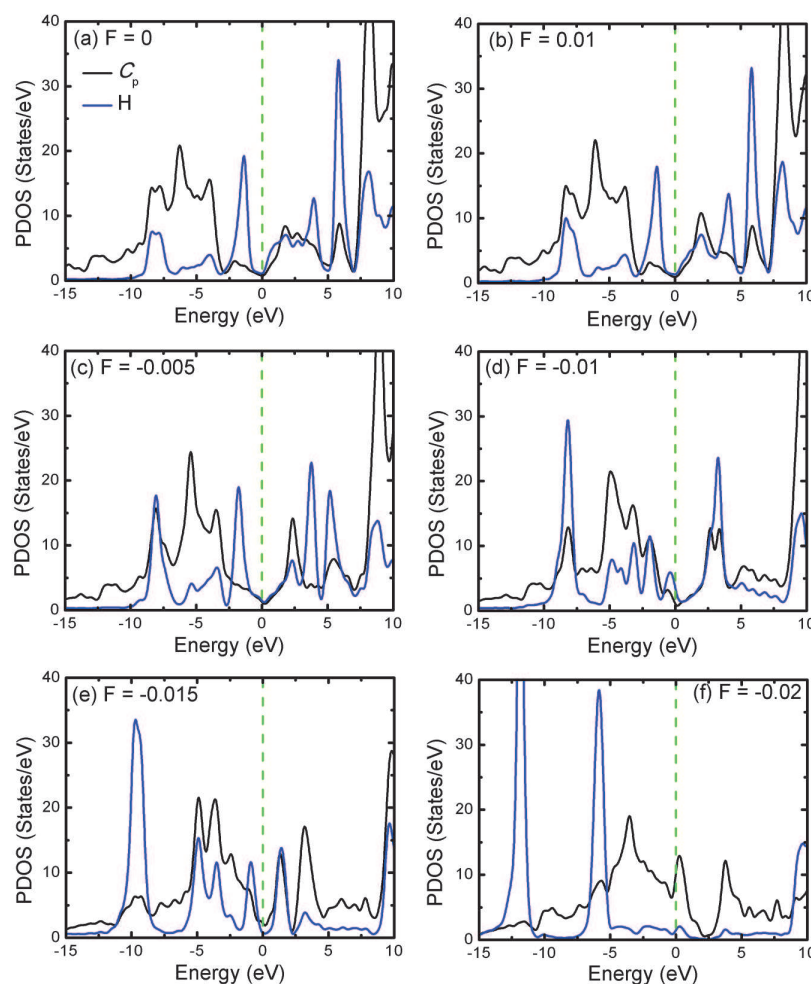


Fig. 3. Partial density of states (PDOS) of the hydrogen and the carbon atoms which are bond with hydrogen in the presences of different electric fields. The black and blue curves are the PDOS of the two H atoms and p orbit of the two C atoms at the transition states. The vertical lines indicate the Fermi level. (Reproduced with permission from Ref. (Ao & Peeters, 2010a). Copyright 2010, AIP)

2.2 Hydrogenation of N-doped graphene

As shown in the last section, the process of hydrogenation in pristine graphene is divided into two steps: molecular hydrogen dissociation under the electric field and the formation of covalent bonds between the dissociated H atoms and C atoms after removing the electric field. This two-step hydrogenation process prevents the efficiency of graphene hydrogenation, and it is desirable to propose a direct hydrogenation approach, i.e. to find a way to reduce both the reaction barrier and reaction energy.

Doping of graphene is usually used to functionalize graphene (Rao et al., 2009). For example, Al-doped graphene was theoretically found to significantly enhance CO adsorption, where CO is found to be chemically adsorbed on the doped Al atom (Ao et al., 2008a). The gas adsorption properties of graphene with other elements, such as N, B and S, were systemically investigated using density functional theory (Dai et al., 2009). Recently, an *ab initio* study of hydrogen interaction with N-doped carbon nanotubes (CNTs) showed that CNTs with nitrogen reduced the energy barrier of hydrogen dissociation from 1.3 eV to 0.9 eV (Zhang & Cho, 2007). In addition, N-doped graphene has been prepared by carrying out arc discharge in the presence of H₂ and pyridine or H₂ and ammonia. Transformation of nanodiamond in the presence of pyridine also yields N-doped graphene (Panchakarla et al., 2009). N-doped graphene can also be synthesized by the chemical vapor deposition method (Wei et al., 2009) and through electrothermal reaction with ammonia (Wang et al., 2009). Therefore, in this section, the pathway for H₂ molecular dissociative adsorption on N-doped graphene under electric field through DFT calculations is investigated.

All DFT calculations are performed with the DMOL3 code (Delley, 1990; 2000), and have the same settings as in section 2.1. The binding energy of an N atom on the graphene layer E_{b-N} is defined as,

$$E_{b-N} = E_{N\text{-graphene}} - (E_{v\text{-graphene}} + E_N) \quad (1c)$$

where $E_{N\text{-graphene}}$, $E_{v\text{-graphene}}$ and E_N are the energy of the system with an N atom doped into the graphene layer, the energy of a pristine graphene layer with a vacancy defect and the energy of a free N atom in the slab, respectively.

2.2.1 The adsorption of hydrogen on N-doped graphene

As reported, the H₂ molecule is weakly adsorbed on pristine graphene, which is the reason why many people paid a lot of attention to modify graphene through doping or using the other methods to enhance the interaction between hydrogen and graphene (Ao et al., 2009; 2010a; Ataca et al., 2009). The energetic favorable adsorption configurations of one H₂ molecule and two H atoms on pristine graphene surface are given in Fig. 1, and the corresponding discussion on the structure changes before and after hydrogenation are also shown in section 2.1. The band structures of pristine graphene, the system of a H₂ molecule physisorbed on graphene, and the system of graphene with 2 H atoms chemically adsorbed are shown in Figs. 4(a), 4(b) and 4(c), respectively. One can clearly see that pristine graphene has a zero band gap as expected (Elias et al., 2009; Rao et al., 2009; Shevlin & Guo, 2009; Sofo et al., 2007). After H₂ molecular adsorption, there is almost no change in the band structure and the zero band gap remains. In fact, it is a simple combination of the band structure of pristine graphene and the H₂ molecule. However, for the band structure of 2 H atoms chemically adsorbed on graphene, the significant changes are found near the Fermi level. It has an indirect band gap of 3.4 eV where the top of the valence band is located at the

M point and the bottom of the conductive band is at the Γ point. The band gap is consistent with that of 3.5 eV for fully hydrogenated graphene – graphane (Sofa et al., 2007). Note that all C atoms are fully bonded and there are no unpaired electrons. Therefore, no net spin exists in this system. For half-hydrogenated graphene as shown in Fig. 3(a) of the Ref. (Zhou et al., 2009b), strong σ -bonds are formed between C and H atoms and the π -bonding network formed by p orbitals of the carbon ring is broken, leaving the electrons in the unhydrogenated C atoms localized and unpaired where spins come out. These spins decrease the band gap energy to 0.43 eV significantly (Zhou et al., 2009a, 2009b). In our case, the two H atoms are dissociative adsorbed on two face-by-face C atoms where all electrons in this system are paired without spins, similar to the status of fully hydrogenated graphene-graphane. The accuracy of such a LDA of the system used here has been verified by many other studies (Yao et al., 2007).

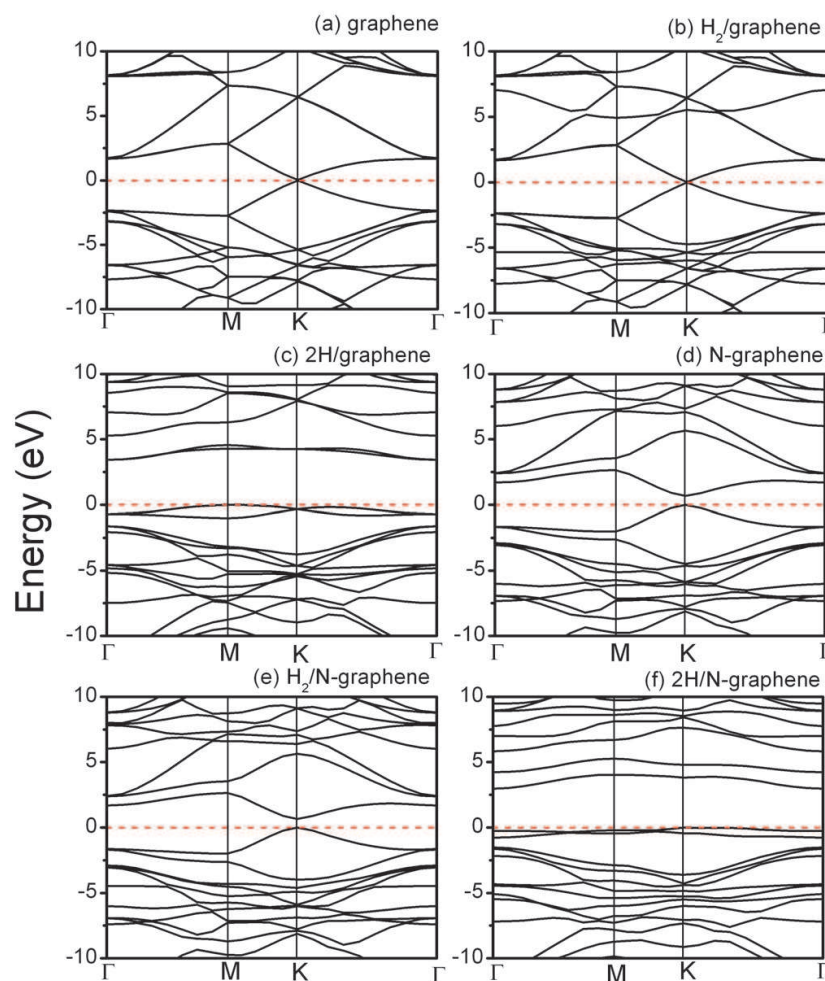


Fig. 4. The band structure of pristine graphene (a), the system with a H_2 molecule adsorbed on pristine graphene (b), the system with 2 H atoms chemically adsorbed on pristine graphene (c), N-doped graphene (d), the system with a H_2 molecule adsorbed on the N-doped graphene (e), and the system with 2 H atoms chemically adsorbed on the N-doped graphene (f). In the figure, a 2×2 supercell of graphene is taken, and the dash lines are the position of the Fermi level. (Reproduced with permission from Ref. (Ao & Peeters, 2010b). Copyright 2010, ACS)

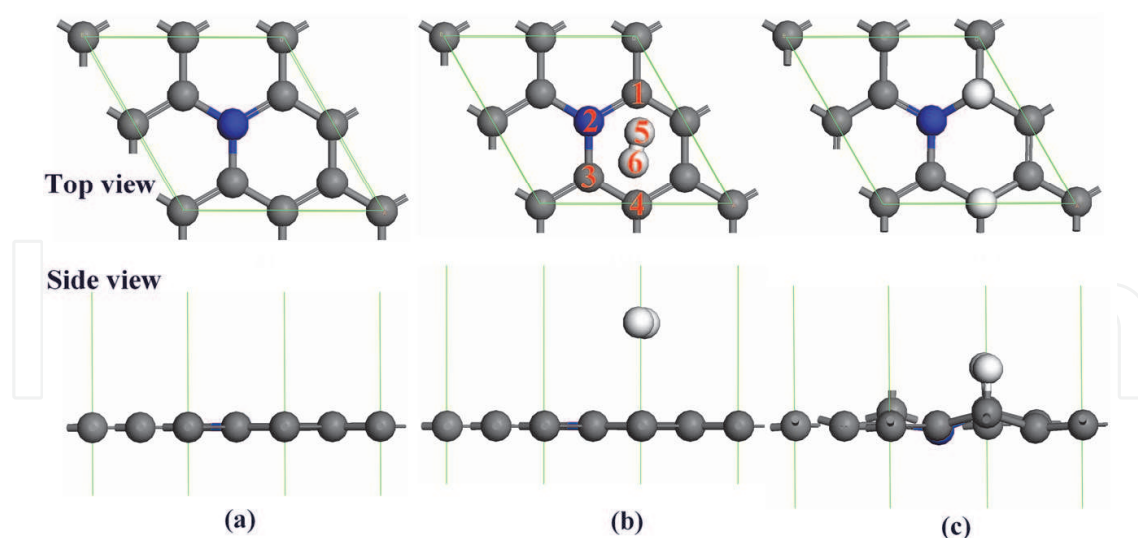


Fig. 5. The atomic structure of the N-doped graphene (a), a H_2 molecule adsorbed on the N-doped graphene (b) and 2 H atoms dissociative adsorbed on N-doped graphene (c). The blue sphere is an N atom. (Reproduced with permission from Ref. (Ao & Peeters, 2010b). Copyright 2010, ACS)

Doping graphene by both electrons and holes changes its electronic structure significantly (Rao et al., 2009). Recently, the nitrogen doped graphene was prepared by arc discharge of graphite electrodes in the presence of H_2 , He, and NH_3 (Panchakarala et al., 2009), chemical vapor deposition (Wei et al., 2009), or through the electrothermal reaction with ammonia (Wang et al., 2009). Furthermore, using *ab initio* calculations, N-doped CNTs was reported to reduce the energy barrier of hydrogen molecule dissociative adsorption (Zhang & Cho, 2007). Therefore, the effect of N doping on the dissociative adsorption of a H_2 molecule is considered. In the experiment, N atoms substitute the C atoms in graphene. The doping concentration can be controlled by adjusting the experimental parameters, such as the ratio among H_2 , He_2 and NH_3 (Panchakarala et al., 2009). In this simulation, a 2×2 supercell for graphene is taken, one of the C atoms is replaced by a N atom, which leads to the ratio of N:C = 1:7. After geometry optimization, the N-doped graphene still keeps the planar feature with a small shrinkage of C-N bond length $l_{C-N} = 1.41 \text{ \AA}$, which $l_{C-C} = 1.42 \text{ \AA}$ in pristine graphene. This is consistent with the other simulation results (Dai et al., 2009). The structure with N doping is shown in Fig. 5(a).

In the arc discharge doping process, the vacancy defects in graphene were induced, thus allowing the N atoms from NH_3 to adsorb at the vacancies and forming the covalent bonds with C atoms (Panchakarala et al., 2009). In this case, the binding energy E_{b-N} between N and graphene layer can be determined by Eq. (1c). It was found that E_{b-N} is as strong as -12.65 eV/atom . For graphite the C-C binding energy was reported to be -9.55 eV/atom (Sofa et al., 2007). Therefore, it is favorable to form N-C bonds in the presence of a N atom, although there is an energy barrier for the reaction, which can be overcome through decalescence or by arc discharge technique in the experiment.

The favorable atomic structure of a H_2 molecule physisorbed on the N-doped graphene is shown in Fig. 5(b). The result shows that the planar structure remains and the adsorbed H_2 molecule is located on the hollow site of the carbon hexagon. The distance $d_{H_2\text{-graphene}}$ and adsorption energy E_{b-H_2} are respectively 2.615 \AA and -0.159 eV , which are similar to the

results above for a H_2 molecule physisorption on pristine graphene. In other words, doping N into graphene has only a little effect on H_2 physisorption.

Different from the aforementioned physisorbed H_2 , the favorable atomic structure of 2 H atoms chemically bonded on the C atoms is given in Fig. 5(c). Similar results for the case of pristine graphene are obtained, where the average binding energy for the C-H bonds E_{b-H} is -2.028 eV and the C atoms binding with the H atoms move upwards by about 0.35 Å. However, the bond lengths for the two C-H bonds l_{C1-H5} and l_{C4-H6} are different; they are 1.122 and 1.132 Å, respectively. Meanwhile, the doped N atom moves downwards with about 0.1 Å. Note that the 2 H atoms were adsorbed at two C atoms that are asymmetric. H5 was adsorbed onto C1, but H6 was adsorbed on C4 not C3 which is symmetric with C1 as shown in Fig. 5(c). To investigate the effect of cell size on the adsorption sites of H atoms on graphene, the cell size is increased to a 4×4 supercell. It was found that the two H atoms still prefer to take the sites of the C atoms near to the N atom.

Fig. 6 shows a H_2 molecule dissociative adsorption pathway on the N-doped graphene. Following the reaction coordinate, the reaction energy barrier is 2.522 eV, which is a little smaller than 2.734 eV for the H_2 molecule dissociative adsorption on pristine graphene. The result is consistent with the report that N doping into CNTs would reduce the energy barrier of molecular hydrogen dissociative adsorption (Zhang & Cho, 2007). Besides the initial and final structures of the reaction, the atomic structure with the minimum energy state, State 1, and the transition state are also given in Fig. 6. For State 1, the H_2 molecule diffuses from the hollow site of the carbon hexagon to a site near the doped N atom before the transition state. For the transition state, the H_2 molecule is already dissociated into 2 H atoms but only H5 is adsorbed on C1 and H6 is a free atom near C4. Subsequently, H6 is also adsorbed as shown in the final structure. Such a reaction pathway explains why the two H atoms are not adsorbed onto two C atoms with symmetry, since the adsorption of the two H atoms does not occur at the same time. The adsorption of the first H atom would change the electronic distribution and also the chemical reactivity of each C atom.

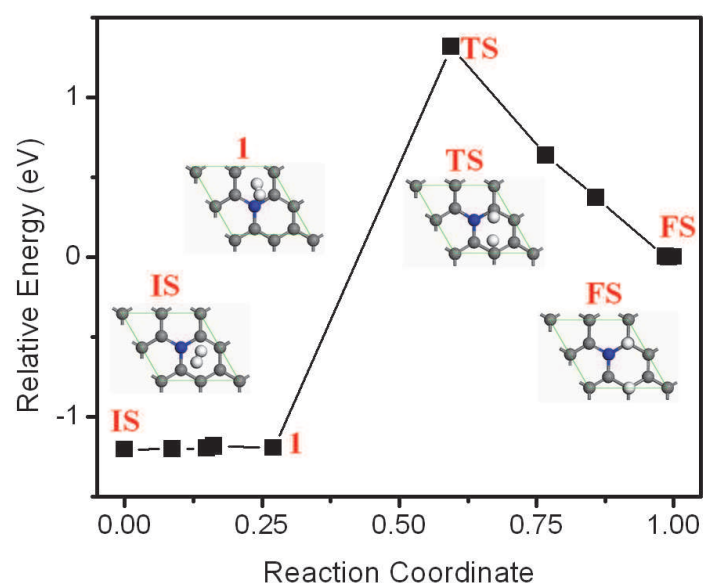


Fig. 6. The reaction pathway of a H_2 molecule dissociative adsorption on a N-doped graphene layer. (Reproduced with permission from Ref. (Ao & Peeters, 2010b). Copyright 2010, ACS)

The band structures of N-doped graphene, the system with a H₂ molecule physisorbed on N-doped graphene, and the system with 2 H atoms chemically adsorbed on N-doped graphene are given in Figs. 4(d), 4(e) and 4(f), respectively. It is clearly shown in Fig. 4(d) that there is an energy gap between the valence and conduction bands at the K point with N doping. The direct band gap is about 0.7 eV. As clarified by the others (Martine et al., 2007), the doping atoms enter into the lattice of graphene, form covalent bonds with the C atoms and change the atomic structure of graphene. This would largely modify the electronic structure of graphene and suppress the density of states near the Fermi level, thus a gap is opened between the valence and conduction bands. After a H₂ molecule is adsorbed, the band structure of the system is not fundamentally changed. However, for the system of 2 H atoms adsorbed on N-doped graphene, the band structure changes a lot and an indirect band gap of around 3 eV is found. The top of the valence band is located at the K point and the bottom of the conduction band is at the Γ point. Therefore, doping N into graphene has no significant effect for the H₂ molecule physisorption and only slightly reduces the dissociation energy barrier. However, for the band structure of graphene, doping N would induce a band gap energy of ~ 0.7 eV. Thus, similar to the N-doped CNTs (Zhou et al., 2006), N-doped graphene exhibits semiconductor behavior, which leads to a decreased conductivity, an improved on/off ratio and a Schottky barrier when electrodes are added.

2.2.2 The effect of an applied electric field on the dissociative adsorption

As a perpendicular electric field F will lead to a polarization of the charge density, it will have an effect on the dissociative adsorption of hydrogen. To investigate the effect of the electric field on the hydrogen dissociation desorption on N-doped graphene, a perpendicular electric field is applied on the N-doped graphene system. The energies of the initial structures, transition structures, final structures, reaction barriers and reaction energies of a H₂ molecule dissociative adsorbed on N-doped graphene under different electric fields are given in Table 1. It is found that the positive electric field reduces the barrier significantly in the N-doped graphene system. When increasing the electric field to $F = 0.009$ a.u. (1 a.u. = 5.14×10^{11} V/m), no barrier is found, the reaction occurs automatically. Note that for $F \geq 0.005$ a.u., the reaction energy is negative in the N-doped system and it decreases as F increases. A negative electric field is also applied in this system, the negative electric field leads to an increase of the energy barrier. It is understandable that reversing the electric field has an opposite effect on the energy barrier for hydrogen dissociative adsorption due to the polarization effect of the electric field. Therefore, Table 2 gives the atomic charges of the two H atoms and the two C atoms which are bound to the two H atoms, at the transition state in the presence of different electric fields in N-doped graphene. As shown in the table, electrons move towards the H atoms with increasing F , while the opposite behavior is found for the two C atoms and the N atom. Thus a positive electric field leads to a transfer of electrons from the bottom atoms to the top atoms and a negative electric field has the opposite effect.

It is interesting to notice that the reaction barrier is negative, i.e. -0.895 eV, for a H₂ molecule dissociative adsorbed on N-doped graphene under a 0.009 a.u. electric field. Therefore, this reaction pathway is shown in Fig. 7. As shown in this figure, there are two transition states TS1 and TS2, and two minimum energy states: State 1 and State 2. For State 1 and State 2, the two dissociative H atoms bond on C1 and C4, which are closest to the doped N atom. For TS1 and TS2, the H₂ molecule is dissociated and only one H atom is bonded with C1, which is closest to the doped N atom. Another H atom is free. However, the positions of the

free H atom are different for the two transition states. The configurations of the two transition states are similar to that in the N-doped graphene system without electric field, where there is also one H atom bonded on C1 and another is free.

	F (a.u.)	Energy of reactant (Ha)	Energy of production (Ha)	Transition state (Ha)	Dissociation barrier (eV)	Reaction energy (eV)
Pristine graphene	0	-303.482	-303.452	-303.382	2.734	0.828
	0	-320.010	-319.966	-319.918	2.522	1.205
N-doped graphene	0.005	-319.924	-319.941	-319.891	0.878	-0.480
	0.009	-319.940	-320.022	-319.973	-0.895	-2.241
	-0.005	-319.903	-319.828	-319.791	3.033	2.046

Table 1. The energies of reactants, productions, transition state, dissociation barriers and reaction energies for the reaction of a H₂ molecule with pristine graphene or with N-doped graphene and 2 H atoms bond on pristine graphene or on N-doped graphene in the presence of different electric fields.

	Atom	$F=-0.005$	$F=0$	$F=0.005$	$F=0.01$
N-doped graphene	H5	0.287	0.126	-0.024	-0.115
	H6	0.226	-0.031	-0.291	-0.402
	C1	-0.293	-0.206	-0.113	-0.071
	C4	-0.264	-0.104	0.008	0.102
	N	-0.414	-0.378	-0.368	-0.346

Table 2. Atomic charge of the two H atoms and the two C atoms which are bonded with the two H atoms, at the transition state under different electric field in N-doped graphene. The different atoms are numbered which are given in Fig. 5. The units of the charge and electric field are $|e|$ and a.u., respectively.

The reaction barrier -0.895 eV is the energy difference between IS and TS2. In this reaction process, there are two barriers that should be overcome, State 1 to TS1 with a barrier of 0.966 eV, and State 2 to TS2 with a barrier of 0.801 eV. However, the energy from the exothermic process of IS to State 1 is sufficient to support the endothermic process from State 1 to TS2. In other words, the dissociative adsorption reaction can occur automatically if the energy created from IS to State 1 can be used to provide the energy needed from State 1 to TS2. Further increasing the electric field beyond 0.009 a.u., no transition state is found and the final structure can be obtained directly even by the geometry optimization method. Therefore, the electric field can induce molecular hydrogen dissociative adsorption in the N-doped graphene system, and the process changes from an endothermic to an exothermic reaction. It means that the electric field and N doping act as the catalyses of H₂ dissociation. The origin of the differences in the energy barrier of hydrogen dissociative adsorption on graphene can be understood through the analysis of the partial density of states (PDOS). Fig. 8 shows the PDOS of the hydrogen and carbon atoms which the H₂ molecule dissociates and is adsorbed on for different electric field. The interaction between the hydrogen and graphene atoms is mainly determined by the bonding and antibonding interactions between

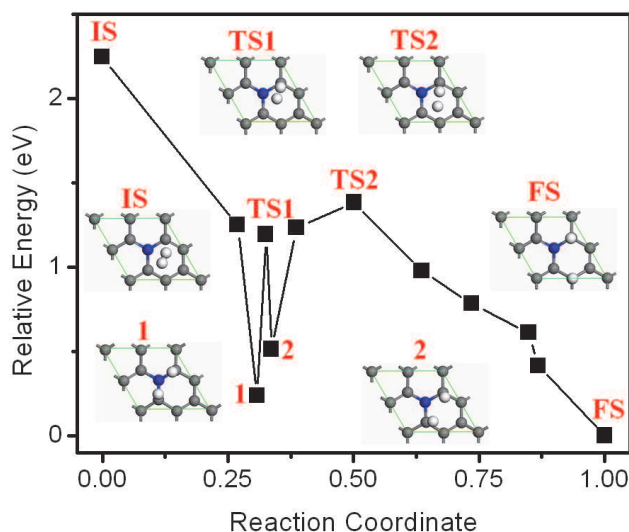


Fig. 7. The reaction pathway of a H_2 molecule dissociative adsorption on N-doped graphene in the presence of an electric field $F = 0.009$ a.u. (1 a.u. = 5.14×10^{11} V/m). In this figure, there are 2 transition states TS1 and TS2. (Reproduced with permission from Ref. (Ao & Peeters, 2010b). Copyright 2010, ACS)

the σ_g and σ_u states of hydrogen and the p state of the carbon atoms directed perpendicular to graphene (p_z) which bond with the hydrogen atoms. The C p_z -band, which participates strongly in bonding with hydrogen, can be identified between the Fermi level and ~ -2 eV in the PDOS of C atoms of isolated graphene. These bands almost disappear in the plots of the PDOS of the C atoms with interaction with H atoms in the 2H/graphene system. Therefore, the strength of the interaction and the trends in the dissociative adsorption energy barriers can be explained by considering the positions and weights of the bonding and antibonding states between the C p_z and hydrogen bands. At the position of the C-H bands, there are distinctive differences in the PDOS of the C atoms with and without H interaction. At the other positions, their PDOS are almost identical. Based on the positions of the bands of C and H atoms, the character of the C-H bands can be easily assigned. The lowest C-H band around -8 eV are obviously due to the interaction of the H σ_g state and C p_z state. The second lowest C-H band around -4 eV is mostly due to the bonding interaction of H σ_u and C p_z states since they are above the H σ_g state. The highest C-H bands are due to a combination of the interaction between the C p_z and H σ_u states, and between the H σ_u and the antibonding C p_z states above the Fermi level. The position and weight of the highest C-H bands determine the strength of the interaction and thus determine the energy barrier heights of the transition states (Zhang & Cho, 2007). As one can see from Figs. 8(a) and 8(b), the third C-H bands correspond to the high energy barrier as shown in Table 1. In Fig. 8(d), the weight of the third C-H band is smallest and this case has the lowest energy barrier while the weight of the third C-H band is the largest in Fig. 8(a) and it has the highest barrier, which agrees with the result in Table 1. When comparing Figs. 8(a) and 8(b), N doping induces a weight increase of the two lowest C-H bands and a weight decrease of the highest C-H band slightly. On the other hand, the presence of an electric field leads to a weight increase of the two lowest C-H bands and a weight decrease of the highest C-H band for the hydrogen dissociative adsorption in the N-doped graphene system. These confirm that N doping and a positive electric field have catalytic effects on hydrogen dissociative adsorption.

The hydrogenated graphene, i.e. graphane, was first synthesized in 2009 by exposing graphene to a hydrogen plasma (Elias et al., 2009). Here, a new promising approach is proposed to hydrogenate graphene. With this technique, the hydrogenation can be realized automatically. The hydrogenated N-doped graphene has two very attractive properties for applications. It has a very high volumetric and gravimetric hydrogen density if fully hydrogenated, and has a band gap around 3 eV. The gravimetric capacity of 7.5 wt% hydrogen is higher than the 6 wt% hydrogen target indicated by the Department of Energy U.S. (DOE), and the volumetric hydrogen capacity of 0.12 kg H₂/L is higher than the DOE target of 0.081 kg H₂/L. Alternatively, the band gap of N-doped graphene is increased to 3 eV after 2 H atoms are adsorbed, i.e. in the range of UV light. This is comparable to TiO₂, graphitic C₃N₄ materials and porous graphene, which have shown the potential applications in photocatalyzed splitting of water into hydrogen (Du et al., 2010; Sum et al., 2002; Wang et al., 2008). These results suggest that the hydrogenated N-doped graphene may solve the band gap problem of graphene for nanoelectronic applications and display photocatalytic activity.

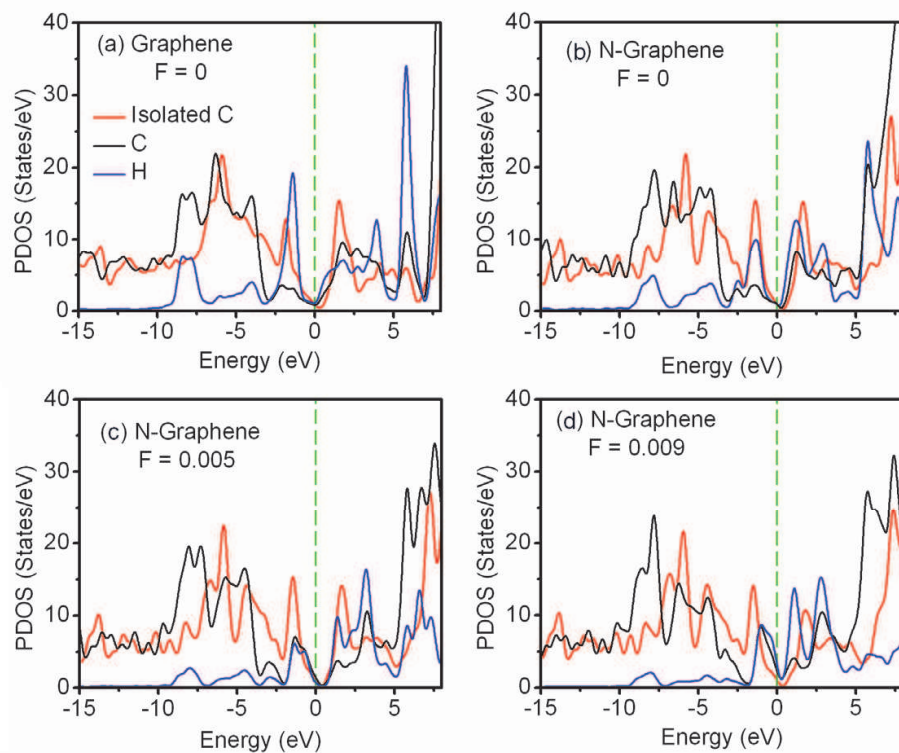


Fig. 8. Partial density of states (PDOS) of the hydrogen and the carbon atoms which are bonded with hydrogen without and with N doping of graphene in the presence of different electric fields. (a) H₂ dissociation over pristine graphene without electrical field. (b) H₂ dissociation over N-doped graphene without electrical field. (c) H₂ dissociation over N-doped graphene with $F = 0.005$ a.u.. (d) H₂ dissociation over N-doped graphene with $F = 0.009$ a.u.. The black and blue curves are the PDOS of the two H atoms and the two C atoms at the transition states, the red curves are the PDOS of the same C atoms in graphene without H, with graphene fixed at the same positions as in the transition states. The vertical lines indicate the Fermi level. (Reproduced with permission from Ref. (Ao & Peeters, 2010b). Copyright 2010, ACS)

3. Diffusion of hydrogen on graphene/graphane interface

As aforementioned, manipulating the edge structure and width of GNR is a way to tuning the electronic properties of graphene, such as opening its band gap. High quality GNRs can be fabricated by selectively hydrogenating graphene or by carving GNRs on a graphane sheet. However, the hydrogen diffusion has a strong influence on the stability of the graphene/graphane interface and such a phenomenon needs to be clarified.

Similar to the studies above, the hydrogen diffusion behavior on the graphene/graphane interface is investigated with DFT calculation and all the DFT calculations were performed using the DMOL3 code (Delley, 2000). The generalized gradient approximation (GGA) with revised Perdew-Burke-Ernzerhof (RPBE) functional was employed as the exchange-correlation functional (Hammer et al., 1999). A double numerical plus polarization (DNP) was used as the basis set, while the DFT semicore pseudopotentials (DSPP) core treatment was employed for relativistic effects that replaces core electrons by a single effective potential. Spin polarization was included in all our calculations. The convergence tolerance of energy was set to 10^{-5} Ha (1 Ha = 27.21 eV), and the maximum allowed force and displacement were 0.02 Ha and 0.005 Å, respectively. To investigate the diffusion pathways of hydrogen atoms at the graphene/graphane interface, linear synchronous transition/quadratic synchronous transit (LST/QST)(Halgren & Lipscomb, 2000) and nudged elastic band (NEB) (Henkelman & Jonsson, 2000) tools in DMOL3 code were used, which have been well validated in order to search for the structure of the transition state (TS) and the minimum energy pathway. In the simulations, three-dimensional periodic boundary conditions were imposed, and all the atoms are allowed to relax.

The supercells used for the zigzag and armchair graphene/graphane nanoribbons are shown in Figs. 9(a) and 9(b), respectively. The interlayer interaction was minimized by allowing a vacuum width of 12 Å normal to the layer. For both type of nanoribbons, the C atoms are displaced from the C plane by about 0.29 Å due to the bonded H atoms. This value is similar to the shift of 0.32 Å that C atoms experience when a H₂ molecule is dissociative adsorption on graphene (Ao & Peeters, 2010a). In both cases, this is a consequence of the change in the hybridization of the C atoms from sp^2 in graphene to sp^3 in graphane. In addition, for the zigzag GGNR both the graphene and the graphane nanoribbons are flat [see Fig. 9(a)]. However, the graphene and graphane layers are not in the same plane, they are connected with an angle of about 162° at the interface, which is consistent with previous reports (Hernández-Nieves et al., 2010; Lu & Feng, 2009). For the armchair GGNR [Fig. 9(b)], the graphene and graphane regions are almost in the same plane, while there is little curvature in the graphene nanoribbon.

Now the stability of the two types of interfaces is analysed by calculating the diffusion barriers for hydrogen atoms. For the case of a zigzag interface, there are two different types of C and H atoms, which are indicated in Fig. 9(a) as sites A and B. For the diffusion of the H atom bonded to the C atom at site A, there are two possible diffusion paths labeled as 1 and 2 in Fig. 9(a). At the site B, there are three possible diffusion pathways for the H atom that we label as 3, 4 and 5. In the case of an armchair interface, all the C atoms at the interface are equivalent from a diffusion point of view. So there are five different diffusions pathways that are labeled as 6-10 in Fig. 9(b). When analysing the diffusion paths, it is found that all the diffusions are along linear pathways, and also that the H atom is free without directly binding to any C atom at the transition state.

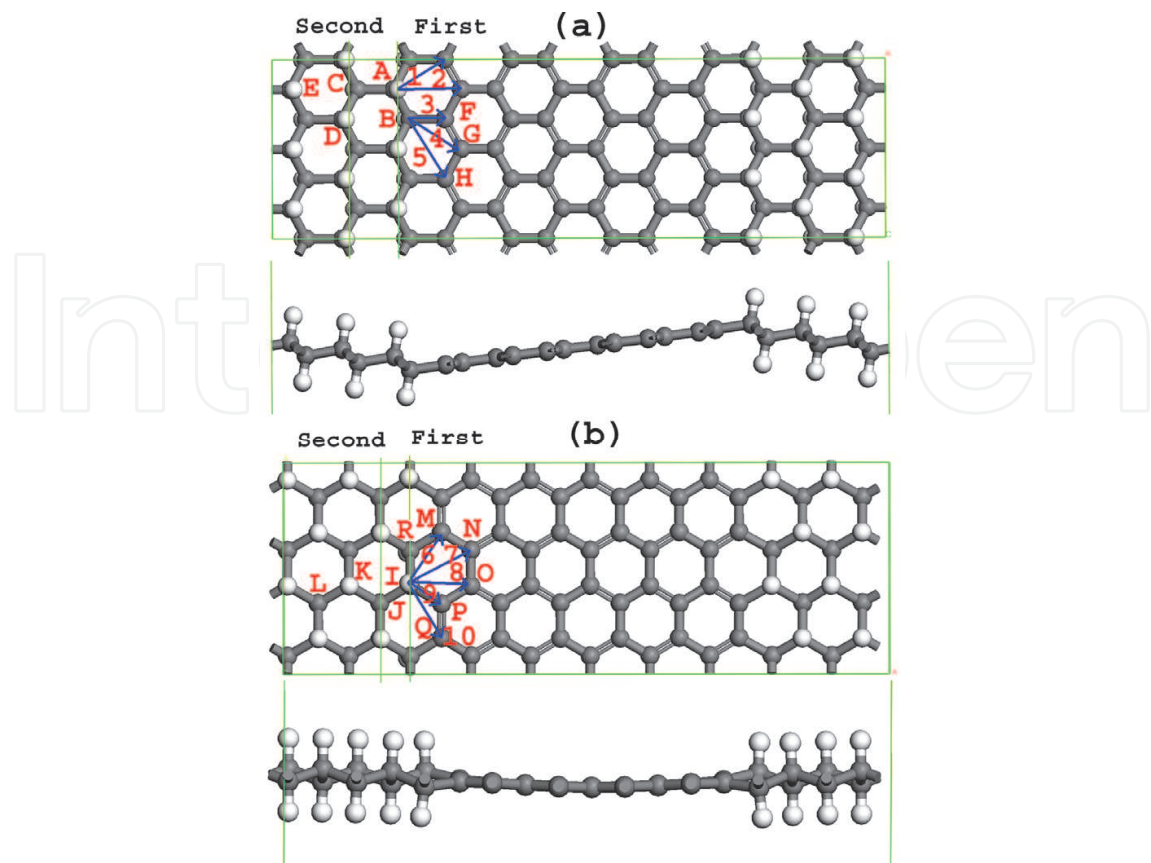


Fig. 9. Atomic structure of graphene/graphane nanoribbons with (a) zigzag and (b) armchair interfaces after relaxation. The arrows indicate the different diffusion pathways considered. The gray and white spheres are C and H atoms, respectively. (Reproduced with permission from Ref. (Ao et al, 2010c). Copyright 2010, AIP)

The diffusion barriers for the different paths and for both types of graphene/graphane interfaces are summarized in Table 3. For the zigzag interface, it is found that the barriers are 3.83, 4.48, 2.86, 3.64 and 3.86 eV for the pathways 1–5, respectively. Thus, the minimum diffusion barrier for the zigzag GGNRs involves H diffusion from the carbon atom at site B along the C–C bond to its nearest carbon atom with an energy barrier of 2.86 eV. For the armchair interface, energy barriers for pathways 6–8 and 10 are 3.17, 4.07, 4.20 and 4.05 eV, respectively. The pathway number 9 involves H diffusion to the nearest C atom at site P. However, it is found that this diffusion cannot occur because during the geometry optimization, the H atom at site P diffuses back to the C atom at site I. Thus, the energy barrier for H diffusion in armchair interfaces can be minimized to 3.17 eV to the second nearest C atom along Path 6.

Recently, it was reported that the diffusion barrier for a single hydrogen atom on pristine graphene layer is about 0.3 eV, which was obtained by DFT calculation using a similar method to this work (Boukhvalov, 2010). Furthermore, the diffusion barriers of transition-metal (TM) atoms on graphene were reported in the range of 0.2–0.8 eV (Krasheninnikov et al., 2009). If the TM adatoms are coupled to a vacancy, the diffusion barrier would increase substantially, reaching to the range of 2.1–3.1 eV. Thus, it was claimed that adatoms with the barrier in such a magnitude are stable at room temperature (Krasheninnikov et al., 2009), supporting the notion that the stability of H atoms at GGNRs interfaces are enhanced greatly and rather stable at room temperature.

	Diffusion pathway	$E_F - E_I$ (eV)	Diffusion barrier (eV)
Zigzag interface	1	1.77	3.83
	2	3.92	4.48
	3	1.90	2.86
	4	1.47	3.64
	5	1.17	3.86
Armchair interface	6	1.39	3.17
	7	2.48	4.07
	8	1.58	4.20
	9 ^a		
	10	1.09	4.05

^a It is found that this diffusion path cannot occur.

Table 3. Diffusion barriers for several diffusion paths and energy differences between the states after and before the diffusion ($E_F - E_I$) in graphene/graphane nanoribbons.

From above analysis, one can see that the minimum diffusion barriers for both of armchair and zigzag interfaces are about one order of magnitude larger than the energy barrier for H diffusion on pristine graphene. From Table 3, one can also see that all the aforementioned H diffusion processes imply increases of several electronic Volts in the energy of the system. At the same time, this indicates that after the diffusion the energy needed for recovering the system back to the initial perfect thermodynamic state is always lower than the energy needed for distorting the interfaces. The barriers for backward diffusion are defined as the difference of energy between the final and the transition states ($E_F - E_T$), and can be obtained from Table 3 as the difference between the values of $E_F - E_I$ and the diffusion barrier ($E_T - E_I$). These demonstrate that the graphene/graphane interfaces are rather stable in both types of hybrid nanoribbons.

Such stability enhancement can be understood by calculating the binding energy of the H atoms in the different conditions, which is proportional to the strength of the C-H bonds. The binding energies (E_b) were calculated by $E_b = E_i - (E_f + E_H)$, where E_i is the initial energy of the system, E_f is the energy of the system after removing the H atom, and E_H is the energy of an isolated H atom. For the zigzag interface, we found that the binding energy of the C-H bond at sites A and B are -4.59 and -2.80 eV, respectively. While for an H atom at site I of the armchair interface, the binding energy is -3.35 eV. All these values are larger than the binding energy of an isolated H atom on a graphene supercell containing 32 C atoms that is equal to -0.88 eV. This indicates the stability enhancement of the H atoms at graphene/graphane interfaces. The results of the binding energies also explains why for the zigzag interface it is easier to move the H atoms from site B ($E_b = -2.80$ eV) than from site A ($E_b = -4.59$ eV). This explanation is also applicable for us to understand why moving the atoms at site B ($E_b = -2.80$ eV) in the zigzag interface is easier than moving the H atoms at site I ($E_b = -3.35$ eV) in the armchair interface. In addition, the C-H bond length at site A (1.108 Å) is smaller than that at site B (1.112 Å). It is believed that if one bond breaks, the remaining coordinated ones would become shorter and stronger (Sun et al., 2009; Zhang et al., 2009). As shown in Fig. 9(a), the C atom at site F binds with other three C atoms, while the C atoms at both sites A and B are bonded with three C atoms and one H atom. Therefore, E_b of C-C bond between sites B and F is greater than that between sites A and B. Such a strong C-C bond weakens the others bonding at site B including the C-H bond (Aizawa et al., 1990).

Hence, the C-H bond at site B is weaker than that at site A. The same explanation can be applicable to the case of armchair GGNR. On the other hand, C-C bond between sites R and I in Fig. 9(b) is weaker than that between sites A and B due to the effect from both C-C bonds between R and M as well as I and P. Thus, the E_b of C-H bond at site I is between those at sites A and B, which is consistent with the DFT result above. Therefore, the H atom at site B can diffuse easier and the GGNR with the armchair interface is more stable than the one with the zigzag interface.

To further understand the mechanism behind of the higher stability of the H atom at site A, the atomic charges are analysed through the Mulliken method. Table 4 gives the atomic charges of atoms near the interfaces. One can see that atoms at both interfaces (i.e. at sites A, B, and I) are more charged than other atoms. At the interface, C atoms are more negative and the corresponding H atoms are more positive. Furthermore, it also shows that the both interfaces mainly affect the charge distribution of the first row of atoms at interfaces, while there is slight effect on the atoms of the second row at the armchair interface. This result agrees with the fact that an interface influences mainly the atoms of the first two rows (Sun, 2007). It is known that the atomic charge is mostly affected by the atoms belonging to the same carbon ring, especially the nearest atoms. For the carbon and hydrogen atoms at the site A, they have similar nearest atoms as the sites in graphane region far apart from the interface, where the three nearest C atoms are bonded by sp^3 orbitals. For the C and H atoms at site B, only two nearest C atoms are bonded by sp^3 orbitals, the other one on its right hand side at site F is bonded by sp^2 orbitals. Therefore, the effect of the interface on site B is

	Atom Site	C atom	H atom
Zigzag interface	A	-0.045	0.045
	B	-0.086	0.057
	C	-0.031	0.033
	D	-0.030	0.033
	E	-0.030	0.031
	F	0.009	
	G	0.019	
	H	0.009	
Armchair interface	I	-0.087	0.063
	J	-0.042	0.038
	K	-0.028	0.033
	L	-0.029	0.031
	M	0.021	
	N	0.005	
	O	0.004	
	P	0.021	
	Q	0.021	

Table 4. Charges of C and H atoms at different sites on the graphene-graphane nanoribbons with different interfaces. The location of the sites is shown in Fig. 9, and the unit of charge is $|e|$.

stronger than that on the site A. On the other hand, for both sites A and B, there are three C atoms bonded by sp^2 orbitals in the carbon ring. Thus, the charge distribution of the atoms on the both sites is affected by the interface. A similar explanation can be applied to the charge difference on the atoms at sites I and J at the armchair interface. Therefore, the C atom at site B (-0.086 $|e|$) is more chemically active than the one at site A (-0.045 $|e|$) because it has more electrons.

4. Conclusion

In summary, the reaction pathways of a H_2 molecule dissociative adsorption on the pristine graphene and the N-doped graphene layer were investigated under a perpendicular applied electric field using DFT calculations. The corresponding atomic and electronic structures of the reactants, productions and transition states were analysed. The results show that the N doping and electric field facilitate the hydrogen dissociative adsorption. The energy barrier for hydrogen dissociative adsorption on N-doped graphene is suppressed by a positive electric field normal to the graphene surface, and the reaction can automatically occur when the electric field is increased above 0.005 a.u.. The origin of the differences in the energy barrier can be understood through the analysis of PDOS. N doping and the applied electric field are considered to diminish the third interaction band between C and H, which mainly determines the barrier height. Based these results, a promising approach to hydrogenate graphene is proposed. It can be used to enhance the hydrogen storage capacity, and also to manipulate the physical properties of graphene for the applications of nanoelectronic devices. Such an exotic phenomenon is associated with its photocatalytic activity due to the band gap opening caused by the applied electric field and doping effects.

On the other hand, the stability of graphene/graphane nanoribbons with both zigzag and armchair interfaces is studied by calculating the diffusion barriers of H atoms using DFT method. It is found that the H atoms can be firmly stabilized by the graphene/graphane interfaces effects. This is resulted by the increase of the C-H bond strength at the graphene/graphane interfaces. The results demonstrate that both zigzag and armchair graphene/graphane interfaces in hybrid nanoribbons are rather stable, thus increasing the feasibility for future technological applications of these systems.

5. Acknowledgement

This study was financially supported by the Vice-Chancellor's Postdoctoral Research Fellowship Program of the University of New South Wales (SIR50/PS19184), the ECR grant of the University of New South Wales (SIR30/PS24201) and ARC Discovery project of DP1096769.

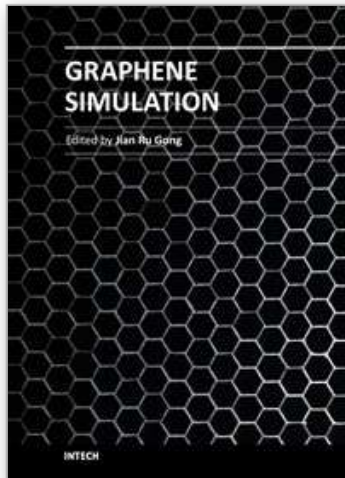
6. References

- Aizawa, T.; Souda, R.; Otani, S.; Ishizawa, Y. & Oshima, C. (1990). Anomalous bond of monolayer graphite on transition-metal carbide surface. *Phys. Rev. Lett.* 64: 768-771.
- Ao, Z. M.; Jiang, Q.; Zhang, R. Q.; Tan, T. T. & Li, S. (2009). Al doped graphene: A promising material for hydrogen storage at room temperature. *J. Appl. Phys.* 105: 074307-074312.

- Ao, Z. M. & Peeters, F. M. (2010a). Electric field: A catalyst for hydrogenation of graphene. *Appl. Phys. Lett.* 96: 253106.
- Ao, Z. M. & Peeters, F. M. (2010b). Electric field activated hydrogen dissociative adsorption to nitrogen-doped graphene. *J. Phys. Chem. C* 114: 14503-14509.
- Ao, Z. M.; Hernández-Nieves, A. D.; Peeters, F. M. & Li S. (2010c). Enhanced stability of hydrogen atoms at the graphene/graphane interface of nanoribbons. *Appl. Phys. Lett.* 97: 233109.
- Ao, Z. M.; Yang, J.; Li, S. & Jiang, Q. (2008a). Enhancement of CO detection in Al doped graphene. *Chem. Phys. Lett.* 461: 276-279.
- Ao, Z. M.; Zheng, W. T. & Jiang, Q. (2008b). The effects of electronic field on the atomic structure of the graphene/ α -SiO₂ interface. *Nanotechnology* 19: 275710.
- Ataca, C.; Aktürk, E. & Ciraci, S. (2009). Hydrogen storage of calcium atoms adsorbed on graphene: First-principles plane wave calculations. *Phys. Rev. B* 79: 041406(R).
- Arellano, J. S.; Molina, L. M.; Rubio, A. & Alonso, J. A. (2000). Density functional study of adsorption of molecular hydrogen on graphene layers. *J. Chem. Phys.* 112: 8114.
- Balog, R.; Jørgensen, B.; Nilsson, L.; Andersen, M.; Rienks, E.; Bianchi, M.; Fanetti, M.; Lægsgaard, E.; Baraldi, A.; Lizzit, S.; Slijivancanin, Z.; Besenbacher, F.; Hammer, B.; Pedersen, T. G.; Hofmann, P. & Hornekær, L. (2010). Bandgap opening in graphene induced by patterned hydrogen adsorption. *Nat. Mater.* 9: 315-319.
- Boukhvalov, D. W. (2010). Modeling of hydrogen and hydroxyl group migration on graphene. *Phys. Chem. Chem. Phys.* 12: 15367-153671.
- Dai, J.; Yuan, J. & Giannozzi, P. (2009). Gas adsorption on graphene doped with B, N, Al, and S: A theoretical study. *Appl. Phys. Lett.* 95: 232105.
- Delley, B. (1990). An all-electron numerical method for solving the local density functional for polyatomic molecules. *J. Chem. Phys.* 92: 508.
- Delley, B. (2000). From molecules to solids with the DMol3 approach. *J. Chem. Phys.* 113: 7756
- Du, A.; Zhu, Z. & Smith, S. C. (2010). Multifunctional porous graphene for nanoelectronics and hydrogen storage: new properties revealed by first principle calculations. *J. Am. Chem. Soc.* 132: 2876-2877.
- Elias, D. C.; Nair, R. R.; Mohiuddin, T. M. G.; Morozov, S. V.; Blake, P.; Halsall, M. P.; Ferrari, A. C.; Boukhvalov, D. W.; Katsnelson, M. I.; Geim, A. K. & Novoselov, K. S. (2009). Control of graphene's properties by reversible hydrogenation: Evidence for graphane. *Science* 232: 610-613.
- Geim, A. K. (2009). Graphene: Status and prospects. *Science* 324: 1530.
- Halgren, T. A. & Lipscomb, W. N. (1977). The synchronous-transit method for determining reaction pathways and locating molecular transition states. *Chem. Phys. Lett.* 49: 225-232.
- Hammer, B.; Hanse, L. B. & Nørskov, J. K. (1999). Improved adsorption energetic within density-functional theory using revised Perdew-Burke-Ernzerhof functional. *Phys. Rev. B* 59: 7413.
- Han, M. Y.; Brant, J. C. & Kim, P. (2010). Electron transport in disordered graphene nanoribbons. *Phys. Rev. Lett.* 104: 056801.
- Henkelman G. & Jonsson, H. (2000). Improved tangent estimate in the nudged elastic band method for finding minimum energy paths and saddle points. *J. Chem. Phys.* 113: 9978.

- Hernández-Nieves, A. D.; Partoens, B. & Peeters, F. M. (2010). Electronic and magnetic properties of superlattices of graphene/graphane nanoribbons with different edge hydrogenation. *Phys. Rev. B* 82: 165412.
- Hyman M. P. & Medlin, J. W. (2005). Theoretical study of the adsorption and dissociation of oxygen on Pt(111) in the presence of homogeneous electric fields. *J. Phys. Chem. B* 109: 6304-6310.
- Jiao, L.; Wang, X.; Diankov, G.; Wang, H. & Dai, H. (2010). Facile synthesis of high-quality graphene nanoribbons. *Nat. Nanotec.* 5: 321-325.
- Koskinen, P.; Malola, S. & Hakkinen, H. (2009). Evidence for graphene edges beyond zigzag and armchair. *Phys. Rev. B* 80: 073401
- Krasheninnikov, A. V.; Lehtinen, P. O.; Foster, A. S.; Pyykkö, P. & Nieminen, R. M. (2009). Embedding transition-metal atoms in graphene: structure, bonding, and magnetism. *Phys. Rev. Lett.* 102: 126807
- Liu, W.; Zhao, Y. H.; Nguyen, J.; Li, Y.; Jiang, Q. & Lavernia, E. J. (2009). Electric field induced reversible switch in hydrogen storage based on single-layer and bilayer graphenes. *Carbon* 47: 3452-3460.
- Lu Y. H. & Feng, Y. P. (2009). Band-gap engineering with hybrid graphane-graphene nanoribbons. *J. Phys. Chem. C* 113: 20841-20844.
- Luo, Z.; Yu, T.; Kim, K.; Ni, Z.; Yu, Y.; You, Y.; Lim, S.; Shen, Z.; Wang, S. & Lin, J. (2009). Thickness-dependent reversible hydrogenation of graphene layers. *ACS Nano* 3: 1781-1788.
- Martins, T. B.; Miwa, R. H.; da Silva, A. J. R. & Fazzio, A. (2007). Electronic and transport properties of Boron-doped graphene nanoribbons. *Phys. Rev. Lett.* 98: 196803.
- Miura, Y.; Kasai, H.; Diño, W.; Nakanishi, H. & Sugimoto, T. (2003). First principle studies for the dissociative adsorption of H₂ on graphene. *J. Appl. Phys.* 93: 3395-3400.
- Novoselov, K. S.; Geim, A. K.; Morozov, S. K.; Jiang, D.; Zhang, Y.; Dubonos, S. V.; Grigorieva, I. V. & Firsov, A. A. (2004). Electric field effect in atomically thin carbon films. *Science* 306: 666-669.
- Okamoto Y. & Miyamoto, Y. (2001). Ab initio investigation of physisorption of molecular hydrogen on planar and curved graphenes. *J. Phys. Chem. B* 105: 3470-3474.
- Panchakarla, L. S.; Subrahmanyam, K. S.; Saha, S. K.; Govindaraj, A.; Krishnamurthy, H. R.; Waghmare, U. V. & Rao C. N. R. (2009). Synthesis, structure, and properties of boron- and nitrogen-doped graphene. *Adv. Mater.* 21: 4726-4730.
- Perdew J. P. & Wang, Y. (1992). Accurate and simple analytic representation of the electron-gas correlation energy. *Phys. Rev. B* 45: 13244.
- Rao, C. N. R.; Sood, A. K.; Subrahmanyam, K. S. & Govindaraj, A. (2009). Graphene: The new two-dimensional nanomaterial. *Angew. Chem. Int. Ed.* 48: 7752-7778.
- Ryu, S.; Han, M. Y.; Maultzsch, J.; Heinz, T. F.; Kim, P.; Steigerwald, M. L. & Brus, L. E. (2008). Reversible basal plane hydrogenation of graphene. *Nano Lett.* 8: 4597-4602.
- Sessi, P.; Guest, J. R.; Bode, M. & Guisinger, N. P. (2009). Patterning graphene at the nanometer scale via hydrogen desorption. *Nano Lett.* 9: 4343-4347.
- Shevlin, S. A. & Guo, Z. X. (2009). Density functional theory simulations of complex hydride and carbon-based hydrogen storage materials. *Chem. Soc. Rev.* 38: 211-225.
- Singh, A. K. & Yakobson, B. I. (2009). Electronic and magnetism of patterned graphene nanoroads. *Nano Lett.* 9: 1540-1543.

- Singh, A. K.; Penev, E. S. & Yakobson, B. I. (2010). Vacancy clusters in graphene as quantum dots. *ACS Nano* 4: 3510-3514.
- Sofo, J. O.; Chaudhari, A. S. & Barber, G. D. (2007). Graphane: A two-dimensional hydrocarbon. *Phys. Rev. B* 75: 153401.
- Sum, K.; Ai-Shahry, M. & Ingler, W. B. (2002). Efficient photochemical water splitting by a chemically modified n-TiO₂. *Science* 297: 2243-2245.
- Sun, C. Q. (2007). Size dependence of nanostructures: Impact of bond order deficiency. *Prog. Solid State Chem.* 35: 1-159.
- Sun, C. Q.; Sun, Y.; Nie, Y. G.; Wang, Y.; Pan, J. S.; Ouyang, G.; Pan, L. K. & Sun, Z. (2009). Coordination-resolved C-C bond length and the C 1s binding energy of carbon allotropes and the effective atomic coordination of the few-layer graphene. *J. Phys. Chem. C* 113: 16464-16467.
- Wang, X.; Li, X.; Zhang, L.; Yoon, Y.; Weber, P. K.; Wang, H.; Guo, J. & Dai, H. (2009). N-doping of graphene through electrothermal reactions with ammonia. *Science* 324: 768-771.
- Wang, X. C.; Maeda, K.; Thomas, A.; Takanabe, K.; Xin, G.; Carlsson, J. M.; Domen, K. & Antonietti, M. (2008). A metal-free polymeric photocatalyst for hydrogen production from water under visible light. *Nat. Mater.* 8: 76-80.
- Wei, D.; Liu, Y.; Wang, Y.; Zhang, H.; Huang, L. & Yu, G. (2009). Synthesis of N-doped graphene by chemical vapor deposition and its electrical properties. *Nano Lett.* 9: 1752-1758.
- Yao, Y.; Ye, F.; Qi, X. L.; Zhang, S. C. & Fang, Z. (2007). Spin-orbit gap of graphene: First-principles calculations. *Phys. Rev. B* 75: 041401.
- Zhang, X.; Kuo, J.; Gu, M.; Bai, P. & Sun, C. Q. (2010). Graphene nanoribbon band-gap expansion: Broken-bond-induced edge strain and quantum entrapment. *Nanoscale* 2: 2160-2163.
- Zhang, Z. & Cho, K. (2007). Ab initio study of hydrogen interaction with pure and nitrogen-doped carbon nanotubes. *Phys. Rev. B* 75: 075420
- Zhou, J.; Wang, Q.; Sun, Q.; Chen, X. S.; Kawazoe, Y. & Jena P. (2009a). Ferromagnetism in semihydrogenated graphene sheet. *Nano Lett.* 9: 3867-3870.
- Zhou, J.; Wu, M. M.; Zhou, X. & Sun, Q. (2009b). Tuning electronic and magnetic properties of graphene by surface modification. *Appl. Phys. Lett.* 95: 103108.
- Zhou, Z.; Gao, X.; Yan, J. & Song, D. (2006). Doping effects of B and N on hydrogen adsorption in single-walled carbon nanotubes through density functional calculations. *Carbon* 44: 939-947.



Graphene Simulation

Edited by Prof. Jian Gong

ISBN 978-953-307-556-3

Hard cover, 376 pages

Publisher InTech

Published online 01, August, 2011

Published in print edition August, 2011

Graphene, a conceptually new class of materials in condensed-matter physics, has been the interest of many theoretical studies due to the extraordinary thermal, mechanical and electrical properties for a long time. This book is a collection of the recent theoretical work on graphene from many experts, and will help readers to have a thorough and deep understanding in this fast developing field.

How to reference

In order to correctly reference this scholarly work, feel free to copy and paste the following:

Zhimin Ao and Sean Li (2011). Hydrogenation of Graphene and Hydrogen Diffusion Behavior on Graphene/Graphane Interface, Graphene Simulation, Prof. Jian Gong (Ed.), ISBN: 978-953-307-556-3, InTech, Available from: <http://www.intechopen.com/books/graphene-simulation/hydrogenation-of-graphene-and-hydrogen-diffusion-behavior-on-graphene-graphane-interface>

INTECH
open science | open minds

InTech Europe

University Campus STeP Ri
Slavka Krautzeka 83/A
51000 Rijeka, Croatia
Phone: +385 (51) 770 447
Fax: +385 (51) 686 166
www.intechopen.com

InTech China

Unit 405, Office Block, Hotel Equatorial Shanghai
No.65, Yan An Road (West), Shanghai, 200040, China
中国上海市延安西路65号上海国际贵都大饭店办公楼405单元
Phone: +86-21-62489820
Fax: +86-21-62489821

© 2011 The Author(s). Licensee IntechOpen. This chapter is distributed under the terms of the [Creative Commons Attribution-NonCommercial-ShareAlike-3.0 License](#), which permits use, distribution and reproduction for non-commercial purposes, provided the original is properly cited and derivative works building on this content are distributed under the same license.

IntechOpen

IntechOpen